Two-point Dixon imaging with flexible echo times and a region growing-based postprocessing algorithm

J. Ma[1]
[1]Imaging Physics, University of Texas MD Anderson Cancer Center, Houston, TX, United States

Introduction: The scan time for a two-point Dixon technique using dual-echo acquisition can become comparable with that for a conventional non-Dixon technique with similar scan parameters (1, 2). Recently, Xiang and Eggers et al. showed that images with echo times that are more flexible than being in-phase and out-of-phase can be used for two-point Dixon processing (3, 4). This increased flexibility can reduce some restriction of scan parameters and further improve the scan efficiency for dual-echo acquisition. However, the critical step of phase correction in postprocessing the images with flexible echo times is based on a statistical iterative process and involves empirical image thresholding (3, 4). Furthermore, modeling of the fat signal assumes a specific linear combination of multiple spectral peaks (5). In this study, we present an alternative postprocessing strategy that uses a generalized signal model and features a fully automated region-growing scheme without a need for image thresholding. Using the proposed postprocessing strategy, we will demonstrate successful water and fat separation with phantom and in vivo images by a 3D dual-echo acquisition with flexible echo times.

Method: The two raw images acquired at echo times TE1 and TE2 are expressed as

$S_1 = \left(W + \delta_1 F e^{i\theta_1}\right)P_1$ [1]; $S_2 = \left(W + \delta_2 F e^{i\theta_2}\right)P_1 P$ [2]

in which W and F represent the amplitudes of water and fat, respectively. (δ_1, δ_2) and (θ_1, θ_2) are the amplitude attenuation factors and chemical shift-related phases of fat at TE1 and TE2 (relative to a TE of 0), respectively. P_1 is the phasor (defined as a complex number with a unit amplitude) of the image S_1 and includes the effects of all of its phase factors (e.g., magnetic field inhomogeneity) except that of the chemical shift of fat. P is an additional phasor of S_2 relative to S_1. For given TE1/TE2, (δ_1, δ_2) and (θ_1, θ_2) can be considered known parameters via precalibration (described below).

Similar to what has been previously described (3, 4), we can calculate the following using Eqs. [1-2]:

$M_1 = (W^2 + \delta_1^2 F^2 + 2\delta_1 WF\cos\theta_1)$ [3]; $M_2 = (W^2 + \delta_2^2 F^2 + 2\delta_2 WF\cos\theta_2)$ [4]

in which $M_1 = |S_1|^2$ and $M_2 = |S_2|^2$. Eqs. [3-4] can be used to derive two sets of possible solutions for W and F: (W_a, F_a) and (W_b, F_b). Using Eqs. [1-2], we can also calculate the following:

$S_1^* S_2 = \left(W + \delta_1 F e^{-i\theta_1}\right)\left(W + \delta_2 F e^{i\theta_2}\right)P$ [5]

Using Eq. [5] as well as (W_a, F_a) and (W_b, F_b), we can calculate:

$A = S_1^* S_2\left(W_a + \delta_1 F_a e^{i\theta_1}\right)\left(W_a + \delta_2 F_a e^{-i\theta_2}\right)$ [6]; $B = S_1^* S_2\left(W_b + \delta_1 F_b e^{i\theta_1}\right)\left(W_b + \delta_2 F_b e^{-i\theta_2}\right)$ [7]

Clearly, the phasor of either A or B will be equal to P depending on whether (W_a, F_a) or (W_b, F_b) is the true physical solution for W and F. Because P is determined by underlying factors (e.g., magnetic field inhomogeneity) that are spatially smooth, we can determine the correct distribution of P by constructing a vector field O (initially set to zero for all of the pixels) that is spatially smooth in its angular orientation and represented by either A or B on a pixel basis. For optimized processing reliability, we adapted a region-growing scheme that was first reported for phase correction in a two-point Dixon technique with in-phase and out-of-phase images (1). As described previously (1), the adapted region-growing process has the following two essential steps:

The first is to calculate two phase differences between A and B for a seed pixel with the projected O for the same seed pixel (conveniently calculated as O averaged in a boxcar neighborhood of the seed). The value of O for the seed pixel will be set either to its A or B depending on which of the two phase differences is smaller. In the second step, two phase differences between A and B for each of the seed's nearest neighbor pixels (whose value of O is still zero) with O of the same seed (averaged again in a boxcar neighborhood) are calculated. The smaller of the two phase differences is then used to decide where the nearest neighbor pixel is stored by comparing the phase difference with its maximum possible range of 0 to π. Among a series of ordered initially-empty pixel stacks, the nearest neighbor pixel will be stored in a high or low ordered pixel stack if the phase difference is large or small, respectively. Once these two steps are completed, a pixel from the lowest ordered nonempty pixel stack is selected as the "best" new seed, and the same two-step processing will be repeated until all of the pixels have served as seeds and been processed.

After O and P are determined by region growing, Eq. [2] can be corrected and then combined with Eq. [1] to easily solve for WP_1 and FP_1. Because P_1 is also expected to be spatially smooth in its angular orientation, WP_1 and FP_1 can be low-pass filtered to obtain $\overline{WP_1}$ and $\overline{FP_1}$ and then the SNR-optimized W and F:

$W = Real\{(WP_1)\,\overline{WP_1}^*/|\overline{WP_1}|\}$ [8]; $F = Real\{(FP_1)\,\overline{FP_1}^*/|\overline{FP_1}|\}$ [9]

Experiment and Results: The proposed postprocessing strategy was implemented using MATLAB (MathWorks) and a 3D fast spoiled gradient-echo bipolar dual-echo pulse sequence was used to collect rawdata for a water/fat phantom (consisting of water and vegetable oil) and for the in vivo abdomen of a human subject using a 1.5T whole-body MR scanner (GE Healthcare; HDxt platform). For the in vivo imaging, an eight-channel phased array body coil was used, and the scan parameters were as follows: TR = minimum, FOV = 36 x 27 cm, acquisition matrix = 256 x 192, flip angle = 12°, slice thickness = 4 mm, total number of slices = 38, and receiver bandwidth = ±83.33 kHz. Minimum as well as different combinations of manually selected echo times were used for the dual-echo readout. For the phantom imaging, an eight-channel phased array head coil and scan parameters similar to those for the in vivo scanning were used except that for a fixed TE1 of 1.2 ms, TE2 varied systematically from 2.9 ms (minimum allowed) to 5.2 ms with a ΔTE of 0.1 ms; for a fixed TE2 of 4.6 ms, TE1 varied systematically from 1.2 ms to 2.9 ms (maximum allowed) with a ΔTE of 0.1 ms.

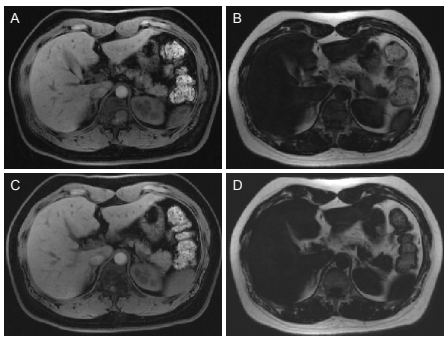

Before Dixon processing, we determined (θ_1, θ_2) as a function of TE by measuring the phase discontinuity between a water-dominant region (e.g., muscle) and an abutting fat-dominant region (e.g., subcutaneous fat). We also determined (δ_1, δ_2) as a function of TE by measuring the image intensity decay of a fixed fat-dominant region. Because fat in different subjects or anatomical locations is known to have very similar compositions, only one in vivo calibration is required to account for the effects of complex fat spectra. Different calibrations may be performed to account for other contributing factors (e.g., vastly different scan protocols or field strengths). The proposed postprocessing strategy was able to reconstruct separate water- and fat-only images of both the phantom and abdomen in vivo for all of the selected TE1/TE2 combinations. For example, the figure at left shows two sets of water- and fat-only images for data acquired at TE1/TE2 = 1.5/3.4 ms with a corresponding precalibrated (θ_1, θ_2) of (77°, 245°) (A, B) and at TE1/TE2 = 2.2/4.4 ms with a corresponding precalibrated (θ_1, θ_2) of (140°, 305°) (C, D) that are closer to being out-of-phase/in-phase. The water/fat separation and overall image quality are excellent in both cases. However, the first set of data required shorter TR and scan times (5.5 ms and 21 s, respectively) than those for the second set of data (6.5 ms and 25 s, respectively) for otherwise identical scan parameters.

Discussion: The proposed region growing-based postprocessing strategy is fully automatic and capable of robust water and fat separation using two input images with flexible echo times. Because of this increased flexibility, we note that the less-efficient dual-echo image acquisition with unipolar flyback readout gradients may be used as a practical alternative to the more-efficient bipolar acquisition for its advantage of having no off-resonance related spatial misregistration between the two input images along the frequency-encode direction.

References: (1). Ma J. MRM 2004;52(2):415-419. (2). Ma J, et al. JMRI 2006;23(1):36-41. (3). Xiang QS. MRM 2006;56(3):572-584. (4). Eggers H, et al. ISMRM, 2010. p. 770. (5). Eggers H. ISMRM 2010. p. 2924.